Hindawi
Modelling and Simulation in Engineering
Volume 2020, Article ID 1453893, 11 pages
https://doi.org/10.1155/2020/1453893

Research Article

Combined Heat and Mass Transfer of Fluid Flowing through Horizontal Channel by Turbulent Forced Convection

Jamal Eddine Salhi,[1] **Kamal Amghar**,[1] **Hicham Bouali**,[2] **and Najim Salhi**[1]

[1]*Laboratory of Mechanics and Energy, Faculty of Sciences, First Mohammed University, Oujda 60000, Morocco*
[2]*Laboratory of Renewable Energy, Embedded System and Information Processing, National School of Applied Science, Agadir, Morocco*

Correspondence should be addressed to Jamal Eddine Salhi; j.salhi@ump.ac.ma and Kamal Amghar; amgharkamaler@gmail.com

Received 20 June 2019; Revised 17 December 2019; Accepted 30 December 2019; Published 28 January 2020

Academic Editor: Dimitrios E. Manolakos

In the present paper, we report a numerical study of dynamic and thermal behavior of the incompressible turbulent air flow by forced convection in a two-dimensional horizontal channel. This one contains the complicated form of the deflector which has been studied by varying the inclination angle from $\varphi = 40^{\circ}$, $\varphi = 55^{\circ}$ to $\varphi = 65^{\circ}$. The baffles are mounted on lower and upper walls of the channel. The walls are maintained at a constant temperature (375 K), the inlet velocity of air is $U_{int} = 7.8$ m/s, and the Reynolds number $Re = 8.73 \times 104$. A specifically developed numerical model was based on the finite-volume method to solve the coupled governing equations and the SIMPLE (Semi Implicit Method for Pressure Linked Equation) algorithm for the treatment of velocity-pressure coupling. For $Pr = 0.71$, the results obtained show that (i) the streamlines and isotherms are strongly affected by the inclinations angles at $Re = 8.73 \times 104$, (ii) the friction coefficient near the baffles increases under the angle exchange effect, and (iii) for a constant Re, the local Nusselt number at the walls of the channel varies with increasing the inclination angle of the deflector. Furthermore, the deflectors are generally used to change the direction of the structure of flow and also to increase the turbulence levels. We can conclude that the contribution of inclined baffles improves the increase of heat and mass transfer in which the Nusselt number at a certain angle increases noticeably.

1. Introduction

In recent decades, heat transfer by turbulent forced convection attracted considerable attention of several researchers. This apply us in industrial domain including cooling of electronic circuit [1], thermal performance of energy efficiency [2], flow and heat transfer in solar collectors [3], lubrication technologies [4], geothermal heat exchangers [5–8] and many others. In the literature, numerous analytical models, numerical and experimental researches have done on the mixed convection heat transfer in different geometries [9, 10]. A literature in this field is widespread by the researchers and very important in industry. According to this literature review, we note that little works have been devoted to study the heat transfer and structure fluid by turbulent forced convection. Several works have used the finite volume method and lattice Boltzmann method (LBM)... etc. to treat the design of heat transfer. Recently, Amghar et al. [11] used a finite volume method and developed analytical expression on the scale analysis to evaluate the heat performance in a horizontal channel. The channel was obstructed by two transversal baffles to study the effect of spacing between the baffles on the heat transfer and flow structure in the case of turbulent forced convection. They found that the heat transfer performance in an exchanger tube increased with the increase in space between the baffles. On the other hand, same authors [12] investigated heat transfer enhancement and fluid flow characteristics through square blocks mounted between two identical isothermal horizontal walls. The authors evaluated the effect of the aspect ratio A/B = 0.5; 0.75; 1 on thermal and hydrodynamic simulations of forced flow along the channel. They concluded that the total heat transfer increases exponentially with increasing the body's aspect ratio. Benzenine et al. [13] reported a numerical study of a three-dimensional laminar forced convection heat transfer process

in a rectangular channel provided with a perforated baffle. They found that the use of a perforated deflector improves the heat transfer (from 0.03% to 82.96%) compared to a solid and simple deflector, which provides economically a very good material reduction (from 5.18% to 82.96%) and mechanically less flow resistance and therefore better performance. In contrast, we can cite Sahel et al. [14] who have examined the design of perforated baffle containing a row of four holes mounted at three different positions along the channel for different Re values (from 10^4 to 10^5); they found an increase in heat transfer with perforated baffle compared to the simple baffle. In this frame, Saim et al. [15] have studied turbulent flow and heat transfer along the horizontal channel arranged periodically on its upper and lower walls by transversal baffles. They concluded that the spacing between baffles affects heat transfer surface between the solid and the fluid in a manner that higher heat transfer is obtained for lower spacing between baffles. In addition, several techniques to achieve the amelioration of heat transfer in solar air collectors reported in the literature have been examined by Menni et al. [16]. Ameur [17] Studied the performance of corrugated deflectors inserted in a rectangular channel heat exchanger. The structure of flow and distribution of the thermal field are determined by numerical simulations. The analysis is made for different angles of baffle varying from 0° to 45°. On the other hand, the ratio h/H is considered for $h/H = 0.4$, 0.5, and 0.6. Then, the expected results showed that an increase in the overall performance factor as a function of the waviness angle growth was noted and that the ratio $h/H = 0.5$ corresponds to the best configuration of the cases studied. Ameur [18] also analyzed the main parameters of design and optimization of a heat exchanger equipped with baffles. The author presented the results concerning, in particular, the effects of the direction and the inclination angle of baffles. The results obtained show the inclination angle of baffles improves the heat transfer. In addition, Boonloi and Jedsadaratanachai [19] conducted a numerical study of heat transfer in the presence of turbulent forced convection of flow in the case of a square channel with discrete combined baffles (DCB), which combined V-baffle and V-orifice. The influence of the flow blocking ratio varied for BR = 0.05, 0.10, and 0.15, and the V-tip directions are examined with a spacing ratio and an angle of attack of 30°, for a Reynolds number between 5000 and 20000. The results obtained are presented in terms of structure of flow and heat transfer. As a result, the insertion of the graded baffle achieved the heat transfer rate about 2.8–6 times compared to the case of the smooth channel. The results show the improvement in the thermal performance factor which reaches an optimum value of about 1.72. Sahel et al. [20] studied the problem of increasing the friction factor that accompanies the insertion of baffles into heat exchangers in order to improve heat transfer throughout the channels. To improve this problem, the authors proposed a new deflector design called "graded baffle" in which they considered two cases: down-/upgraded height of baffles. The authors have explored numerically the effect of aspect ratio of the graded baffle on thermal and hydrodynamic performances. From the predicted results it was found that the new design of baffles provides an adequate reduction in friction factors. The analysis was done for a range of Reynolds numbers from 10^4 to 2×10^4. They showed that the proposed geometry of graded baffle has an important effect on structure of flow and heat transfer throughout the channel. Ameur and Menni [21] analyzed the pressure loss resulting from the equipment of the heat exchangers from baffles, in order to obtain an improvement of the heat transfer and an optimization of the characteristics of a hydrothermal exchanger. The authors have chosen a type of tube exchanger (THE). Therefore, the authors proposed the introduction of circular perforations in the integrated baffle. The flow fields and the thermal characteristics of the heat exchanger are studied. The results obtained show the interest of perforated deflectors and their primary role in the geometrical optimization of heat exchangers, as well as the increase of thermal performance and reduction of the pressure loss.

The main objective of this work is to study a new design along the horizontal channel with complicated form baffles and to investigate numerically thermal and hydrodynamic comportment. Results presented in this paper are obtained from several inclination angles. All numerical results are calculated on a computer with the Core 5 Duo processor of 4 GHz CPU. The content of the paper is structured as follows: In Section 2, we present the mathematical formulation of the physical problem while describing the turbulent forced convection and boundary conditions of the heat exchanger. The numerical analysis is presented in Section 3 with the enrichment functions used in the finite volume method. Section 4 presents the code validation and the numerical results in which the results are presented in terms of streamlines, isotherms, local Nusselt number, profiles of velocity, and friction coefficient. Finally, conclusions of the numerical study are presented in Section 5. The new approach is shown to enjoy the expected accuracy as well as the robustness. Finally, Section 5 concludes this paper.

2. Problem Formulation

2.1. Physical Model. The physical model of the present problem is a horizontal plane channel with two baffles placed on the upper and lower channel walls as shown in Figure 1(a). The upper and lower walls are maintained at the constant temperature ($T_w = 375$ K), and the baffles are supposed to be adiabatic. The dimensions of the physical parameters are illustrated in Table 1. The working fluid is air and its physical properties are assumed constant. The air enters the channel at an inlet temperature T_{int}, inlet velocity U_{int}, and atmospheric pressure. In the present analysis, two-dimensional steady turbulent flow of air is considered. Mathematical formulation of the physical problem is based on some following assumptions:

(i) The problem is considered two dimensional and steady

(ii) The air flow is assumed to be turbulent

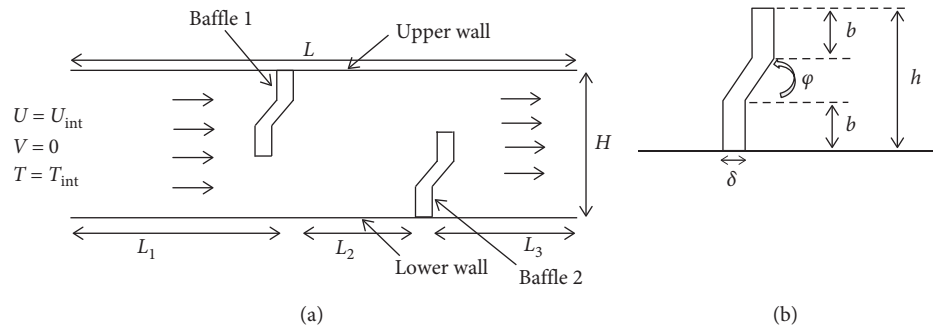

Figure 1: (a) Schematic of the physical model in the (x, y) plane. (b) Baffle dimensions: $b = 0.03$ m.

Table 1: Dimensions of physical problem.

Unit (m)	L	H	h	L_1	L_2	L_3	δ
	0.554	0.146	0.08	0.218	0.142	0.174	0.01

(iii) The fluid air ($\mathrm{Pr} = 0.7$) is a constant physical property and maintained at a constant temperature $T_{\mathrm{int}} = 300$ K

(iv) The fluid is Newtonian and incompressible

(v) The axial velocity and temperature at the entrance of the channel are uniform

(vi) The walls (upper and lower) are maintained at constant temperature

(vii) The heat transfer by radiation is negligible

The dimensions and arrangement of the baffle are shown in Figures 1(a) and 1(b).

These dimensions of physical problem have been considered as the dimensions of experimental study of Demartini et al. [22] for the same geometry, as illustrated in Figure 1.

2.2. Mathematical Formulation. Based on the above assumptions, we can present the mathematical formulation of heat and mass transfer by turbulent forced convection in the horizontal channel as follows:

(i) Conservation of continuity:

$$\frac{\partial(\rho v)}{\partial x} + \frac{\partial(\rho v)}{\partial y} = 0. \tag{1}$$

(ii) Conservation of momentum in x-direction:

$$\frac{\partial(\rho u^2)}{\partial x} + \frac{\partial(\rho uv)}{\partial y} = -\frac{\partial P}{\partial x} + \frac{\partial}{\partial x}\left[(\mu_l + \mu_t)\left(\frac{\partial u}{\partial x}\right)\right] + \frac{\partial}{\partial y}\left[(\mu_l + \mu_t)\left(\frac{\partial u}{\partial y}\right)\right]. \tag{2}$$

(iii) Conservation of momentum in y direction:

$$\frac{\partial(\rho uv)}{\partial x} + \frac{\partial(\rho v^2)}{\partial y} = -\frac{\partial P}{\partial y} + \frac{\partial}{\partial x}\left[(\mu_l + \mu_t)\left(\frac{\partial v}{\partial x}\right)\right] + \frac{\partial}{\partial y}\left[(\mu_l + \mu_t)\left(\frac{\partial v}{\partial y}\right)\right]. \tag{3}$$

(iv) Conservation of energy:

$$\frac{\partial(\rho uT)}{\partial x} + \frac{\partial(\rho vT)}{\partial y} = \frac{\partial}{\partial x}\left[\left(\mu_l + \frac{\mu_t}{\sigma_T}\right)\left(\frac{\partial T}{\partial x}\right)\right] + \frac{\partial}{\partial y}\left[\left(\mu_l + \frac{\mu_t}{\sigma_T}\right)\left(\frac{\partial T}{\partial y}\right)\right]. \tag{4}$$

The turbulence model k-ε is chosen to treat fluid turbulence with a high Reynolds number, while the model composed of two transport equations for k (turbulent kinetic energy) and ε (dissipation rate ε), Launder and Spalding [23] and Shih et al. [24], can be written as follows:

(i) The turbulent energy equation:

$$\frac{\partial(\rho uk)}{\partial x} + \frac{\partial(\rho vk)}{\partial y} = \frac{\partial}{\partial x}\left[\left(\mu_l + \frac{\mu_t}{\sigma_k}\right)\left(\frac{\partial k}{\partial x}\right)\right] + \frac{\partial}{\partial y}\left[\left(\mu_l + \frac{\mu_t}{\sigma_k}\right)\left(\frac{\partial k}{\partial y}\right)\right]. \tag{5}$$

(ii) The turbulent dissipation equation:

$$\frac{\partial(\rho u\varepsilon)}{\partial x} + \frac{\partial(\rho v\varepsilon)}{\partial y} = \frac{\partial}{\partial x}\left[\left(\mu_l + \frac{\mu_t}{\sigma_\varepsilon}\right)\left(\frac{\partial \varepsilon}{\partial x}\right)\right] + \frac{\partial}{\partial y}\left[\left(\mu_l + \frac{\mu_t}{\sigma_\varepsilon}\right)\left(\frac{\partial \varepsilon}{\partial y}\right)\right], \tag{6}$$

where μ_{t} is the turbulent viscosity:

$$\mu_{\mathrm{t}} = \rho c_\mu \frac{k^2}{\varepsilon}. \tag{7}$$

The equations contain three constant values: C_μ, σ_k, and σ_ε, which are mentioned as follows:

$$C_\mu = 0.09,$$
$$\sigma_k = 1.00, \quad (8)$$
$$\sigma_\varepsilon = 1.3.$$

The main parameters for the current investigation are Reynolds number (Re), friction factor (C_f), and local Nusselt number (Nu).

The Reynolds number for the rectangular channel, calculated with the hydraulic diameter of the channel, $D_h = 0.167$ m, and the inlet velocity, $U_{int} = 7.8$ m/s, is taken according to the experiments of Demartini et al. [22], with $\mathrm{Re} = 8.73 \times 104$. This dimensionless parameter is defined by

$$\mathrm{Re} = \frac{\rho U D_h}{\mu}, \quad (9)$$

where ρ is the density of air, μ is the dynamic viscosity, U is the average velocity of air, and D_h is the diameter of the channel.

The friction coefficient is given by

$$C_f = \frac{\tau_w}{(1/2)\rho U^2}, \quad (10)$$

where τ_w represents the shear stress at the wall and U represents the average axial velocity at the section.

The local Nusselt number is defined as

$$\mathrm{Nu} = \frac{h_x \times L}{\lambda_f}, \quad (11)$$

where λ_f and L are the thermal conductivity of fluid and the location at position along the channel, respectively. The local surface heat transfer coefficient h_x is defined as

$$h_x = \frac{Q}{(T_w - T_b)}, \quad (12)$$
$$T_b = T_{ave.air},$$

where T_b, the bulk temperature of fluid, is calculated as

$$T_b = \frac{\int_A U(x,y) T(x,y) \mathrm{d}A}{\int_A U(x,y) \mathrm{d}A}, \quad (13)$$

where A is the fluid flow cross section.

The resolution of equations (1)–(6), obtained previously, requires that we introduce the boundary conditions for each dependent variable. In this work, the conditions at the hydrodynamic and thermal limits of the system are chosen based on the experimental works of the authors in [22, 25].

2.3. Boundary and Interfacial Conditions. The boundary conditions for the dimensionless equations applied to the physical system are formulated as follows:

(a) At the inlet ($x = 0$ and $0 \le y \le H$):

$$U = U_{int},$$
$$V = 0,$$
$$T = T_{int}, \quad (14)$$
$$k_{int} = 0.005\, U_{int}^2,$$
$$\varepsilon_{int} = 0.1\, k_{int}^2.$$

(b) At the heated walls (upper and lower):

$$U = V = 0,$$
$$T = T_w, \quad (15)$$
$$\varepsilon = k = 0.$$

(c) At the solid liquid interface:

$$\lambda_f \frac{\mathrm{d}T_f}{\delta n}\Big]_{\overrightarrow{N}} = \lambda_s \frac{\mathrm{d}T_s}{\delta n}\Big]_{\overrightarrow{N}}, \quad (16)$$
$$T_f\big|_{\overrightarrow{N}} = T_s\big|_{\overrightarrow{N}},$$

where $\overrightarrow{N}$ is the coordinate normal to the interface and λ_f and λ_s are thermal conductivity of fluid and solid.

(d) At the outlet ($x = L$ and $0 \le y \le H$), the gradient of all parameters is zero:

$$\frac{\partial \phi}{\partial x} = 0, \quad \phi = U, V, T, k, \varepsilon, \quad (17)$$
$$P = P_{atm}.$$

3. Numerical Simulation

3.1. Grid Independence Study. The governing equations' system obtained with the associated boundary conditions is solved numerically by the finite volume method. The velocity-pressure coupling is processed using the SIMPLE algorithm developed by Patankar [26]. However, the terms of convection and diffusion in the governing equation are discretized, respectively, by center scheme and QUICK scheme [27], and this last one is considered as a higher-order scheme. After a simplified calculation, we obtain the following discretization equation:

$$a_P \phi_P = a_E \phi_E + a_W \phi_W + a_N \phi_N + a_S \phi_S + a_{EE} \phi_{EE} + a_{WW} \phi_{WW} + a_{NN} \phi_{NN} + a_{SS} \phi_{SS} + \int_v S \mathrm{d}v, \quad (18)$$

where

$$\begin{cases} a_E = D_e - \frac{3}{8}\alpha_e F_e + \frac{1}{8}(1-\alpha_w)F_w + \frac{6}{8}(1-\alpha_e)F_e, \\ a_W = D_w + \frac{1}{8}\alpha_e F_e + \frac{6}{8}\alpha_w F_w - \frac{3}{8}(1-\alpha_w)F_w, \\ a_N = D_n - \frac{3}{8}\alpha_n F_n + \frac{1}{8}(1-\alpha_s)F_s + \frac{6}{8}(1-\alpha_n)F_n, \\ a_S = D_s + \frac{1}{8}\alpha_n F_n + \frac{6}{8}\alpha_s F_s - \frac{3}{8}(1-\alpha_s)F_s, \\ a_{EE} = -\frac{1}{8}(1-\alpha_e)F_e, \end{cases} \quad (19)$$

with $\phi = u, v, T, k, \varepsilon$.

So, in this section, we are interested to study the stability of the axial velocity u; nonuniform grid is used in both x and y directions for all computations. For this, we can choose the number of cells (265×150) to discretize physical model in this problem according to two directions (in x and y directions, respectively) in view of saving computation time. This mesh is more refined in regions with high gradients (of temperature and velocity), i.e., near the solid-fluid interface and near the baffles. Several grids were tested to verify that the solution is mesh size independent (see Table 2). The same mesh system was used for all cases. The convergence criterion is that the normalized residuals are less than 10^{-7} for the flow equations and 10^{-9} for the energy equation.

3.2. Code Validation. Our numerical code is validated by the experimental results obtained by Demartini et al. [22] in the case of rectangular channel with baffle plates. For that, the comparison was made by considering a Reynolds number equal to 8.73×10^4. However, we compare the average axial velocity profiles for two particular positions (upstream of the first baffle at $x = 0.159$ m), as shown in Figures 2 and 3, respectively. These results show that there is a very good agreement between our numerical results and the experimental results of Demartini. However, the validation of the experimental model by our numerical code can confirm the reliability of our numerical results.

4. Results and Discussion

4.1. Streamlines and Isotherms. Forced convection in a channel with baffle plates was studied numerically for high Reynolds number. Streamlines are presented for three inclination angles of two plate baffles of $\varphi_1 = 40^\circ$, $\varphi_2 = 55^\circ$, and $\varphi_3 = 65^\circ$ (see Figure 4). Verification of the hydrodynamic field along the channel is performed, and these show that the presence of baffles in the channel causes several recirculation depending on the velocity intensity (low or high). Furthermore, the values of velocity are very low around the baffles, especially in the downstream zone, and this is caused by the presence of the recirculation. Therefore, as there is a change in the fluid flow, it is observed that high fluid flow disturbance is obtained upstream of the second baffle which induces a rapid change in the direction of flow. Negative velocities are also observed upstream the first baffle approaching the second deflector.

We deduce that the dynamic results for the different values of inclination angles (cases a, b, and c) show the

Table 2: Results for grid test on velocity u.

Mesh	X (m)	Y (m)	u_{max} (m/s)
82×30	0.554	0.160	32.42
180×76	0.554	0.160	34.39
219×122	0.554	0.160	34.53
233×138	0.554	0.160	34.55
265×150	0.554	0.160	34.56

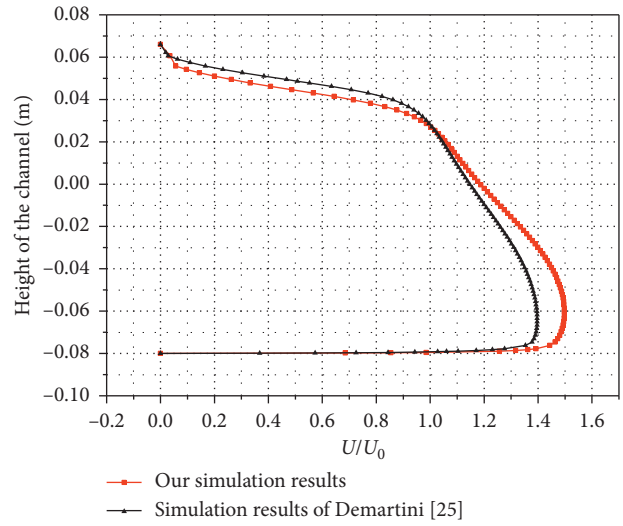

Figure 2: Axial velocity upstream of the first baffle at $x = 0.159$ m.

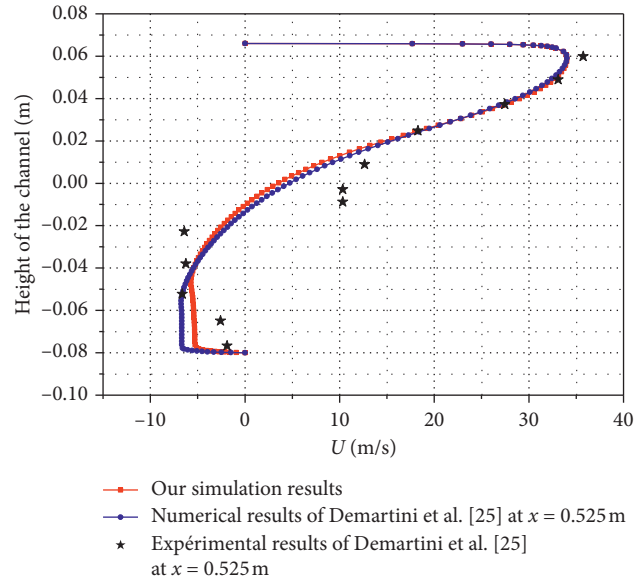

Figure 3: Axial velocity downstream of the second baffle at $x = 0.525$ m.

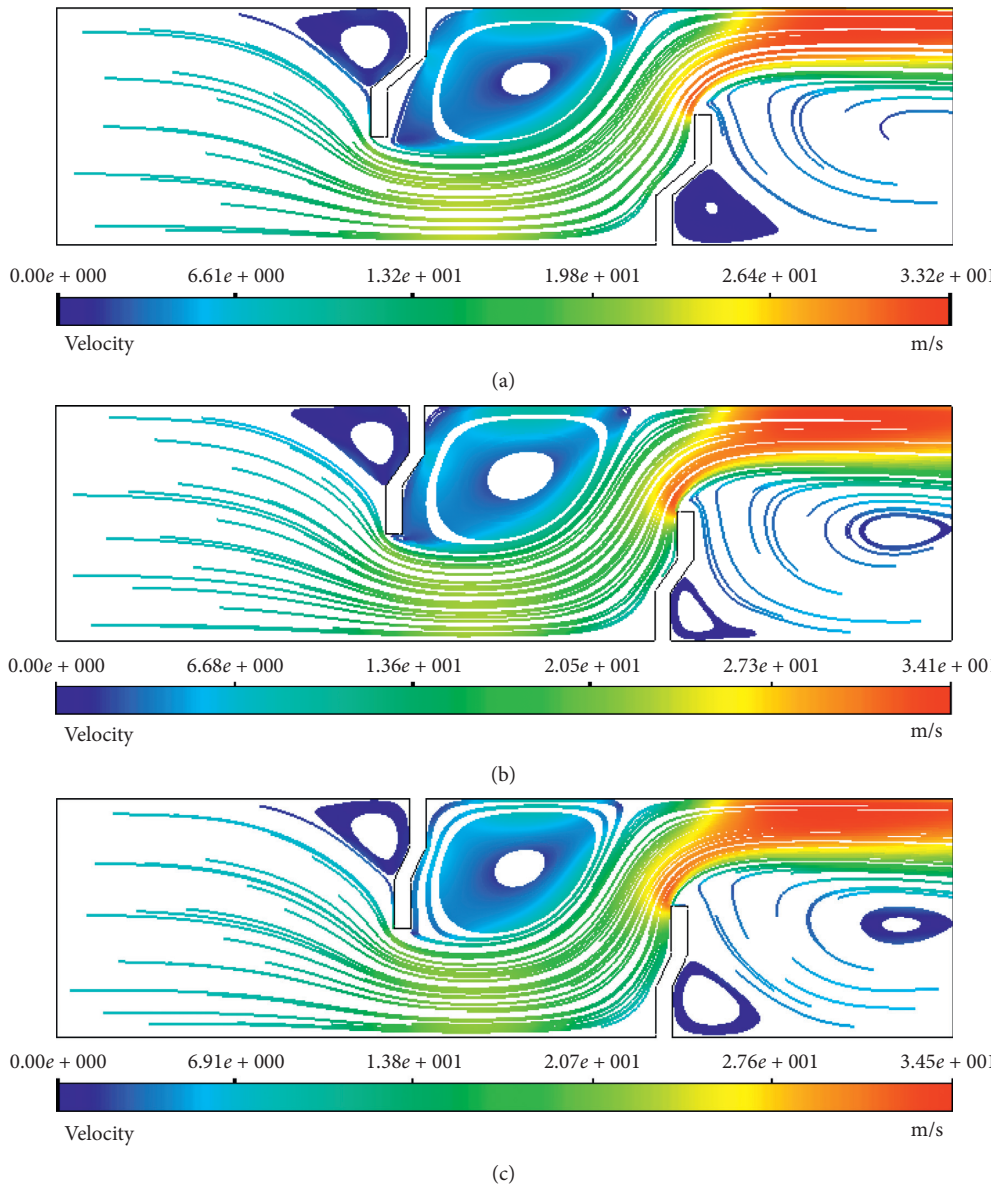

Figure 4: Streamlines for different values of inclination angles: (a) $\varphi_1 = 40^\circ$; (b) $\varphi_2 = 55^\circ$; (c) $\varphi_3 = 65^\circ$.

existence of several areas in the channel. Indeed, we observe three recirculation zones before and after the baffles. In the first zone, which is located just upstream of the first baffle, the fluid is accelerated and arrives with an axial direction velocity (parabolic profile), and as it approaches the latter, the streamlines are deflected. In the second zone, which is located above the baffles, the flow is accelerated by the reduction effect of the passage sections and the third zone, which is located downstream of the baffles. The streamlines are manifested by the effect of the expansion of the flow exiting the section formed by the baffles and walls. The most important phenomenon in this area is the recirculation formation of the flow extent of which is proportional to the angle of inclination. In addition, we observe that in the case of $\varphi_3 = 65^\circ$, the number of vortices is larger and the number of recirculation is more important. Moreover, the recirculation area becomes fully developed and larger than in the previous two cases.

Finally, we conclude that the increase of inclination angle leads to an acceleration of the flow and an increase in fluid velocity and recirculation zones. Indeed, these recirculation zones have a significant effect on heat exchange instability along the channel. Let us note that recirculation zones allow a local improvement of heat transfer; hence, they reveal the importance of using inclined baffles.

Patterns of isotherms at a high Reynolds numbers $\mathrm{Re} = 8.73 \times 10^4$ are been presented in Figure 5 for $\varphi_1 = 40^\circ$; $\varphi_2 = 55^\circ$; and $\varphi_3 = 65^\circ$ in the case of a channel with two inclined baffles. In fact, the fluid is diverted towards the walls of the channel, as shown by the recirculation zones upstream and downstream of two baffles.

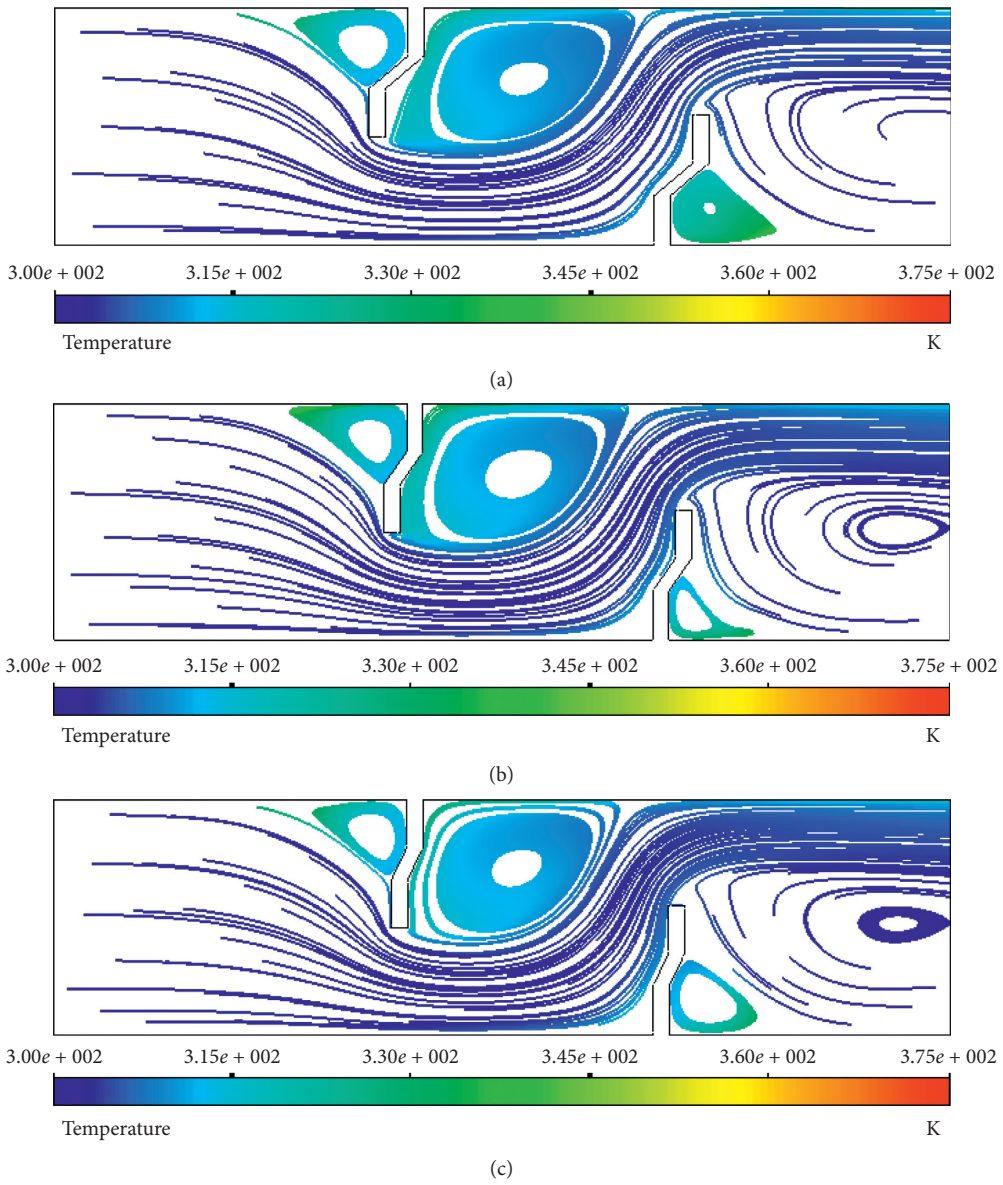

FIGURE 5: Isotherms for different values of inclination angles: (a) $\varphi_1 = 40^\circ$; (b) $\varphi_2 = 55^\circ$; (c) $\varphi_3 = 65^\circ$.

From these figures, the air temperature in the recirculation zones before and after the baffles is significantly high. However, it is confirmed that the case (c) is performed in which the increase in the inclination angle affects the heat transfers from the walls (upper and lower) to fluid air along the channel. In particular, the hottest areas are located near the walls and around the baffles, due to the effects of the presence of vortices that stimulate heat exchange between the air and the heated walls. So, we concluded that the orientation of the baffles improves heat transfer by convection in the considered channel.

4.2. Profiles of Fluid Flow. The velocity variation for the three cases is clearly visible on the contours and on their values that have positive and negative values. To study this evolution of axial velocity along the channel with different values of inclination angles (cases a, b, and c), we have depicted the curves of variation of the axial velocity resulting from this hydrodynamic study for five positions: $x = 0.159$ m, $x = 0.285$ m, $x = 0.315$ m, $x = 0.345$ m, and $x = 0.525$ m.

We observe that at upstream of the first baffle (position: $x = 0.159$ m) and in the lower zone of the channel at downstream of it (position: $x = 0.285$ m), the axial velocity profiles are almost identical for the three cases of angles treated (see Figures 6 and 7). On the other hand, in the upper part of the channel at downstream of the first baffle, the axial velocity profiles are completely different. It is also noted that in the upper part of the channel, we notice negative velocity values appear in the area between the positions of the two baffles with the presence of a recirculation zone. In this area, the reduction in the inclination angle of the baffle leads to an increase in the value of the axial velocity in both directions (positive and negative).

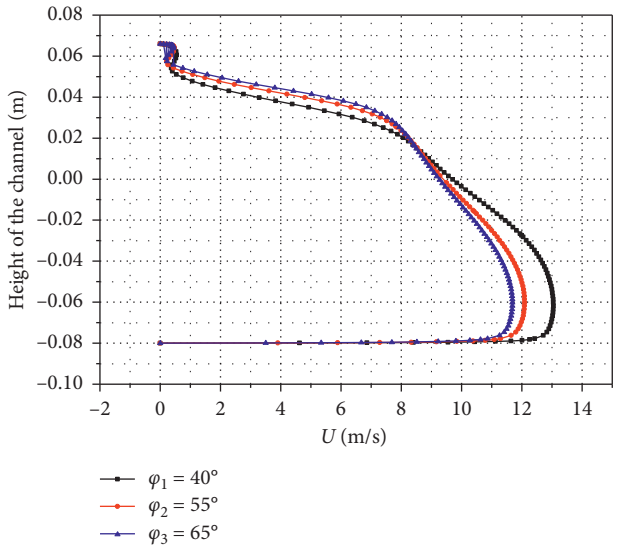

Figure 6: Axial velocity profiles upstream of the first baffle at $x = 0.159$ m for different values of inclination angles: $\varphi_1 = 40^\circ$; $\varphi_2 = 55^\circ$; $\varphi_3 = 65^\circ$.

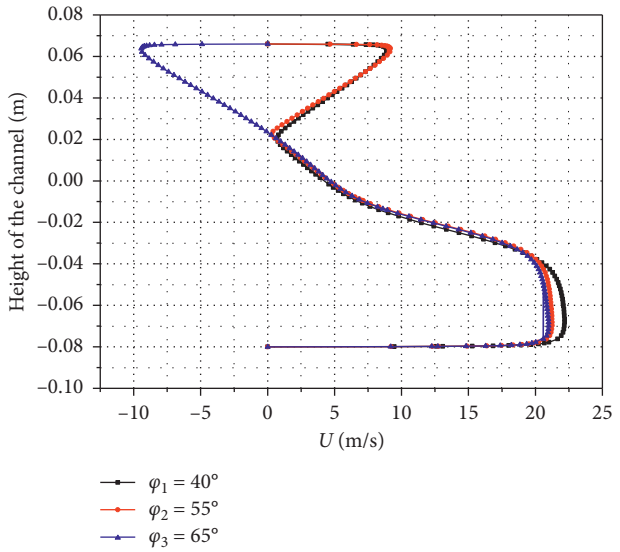

Figure 7: Axial velocity profiles downstream of the first baffle at $x = 0.285$ m for different values of inclination angles: $\varphi_1 = 40^\circ$; $\varphi_2 = 55^\circ$; $\varphi_3 = 65^\circ$.

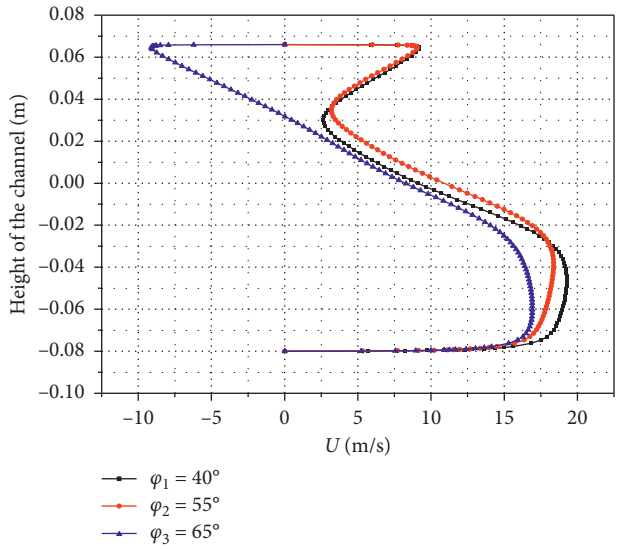

Figure 8: Axial velocity profiles upstream of the second baffle at $x = 0.315$ m for different values of inclination angles: $\varphi_1 = 40^\circ$; $\varphi_2 = 55^\circ$; $\varphi_3 = 65^\circ$.

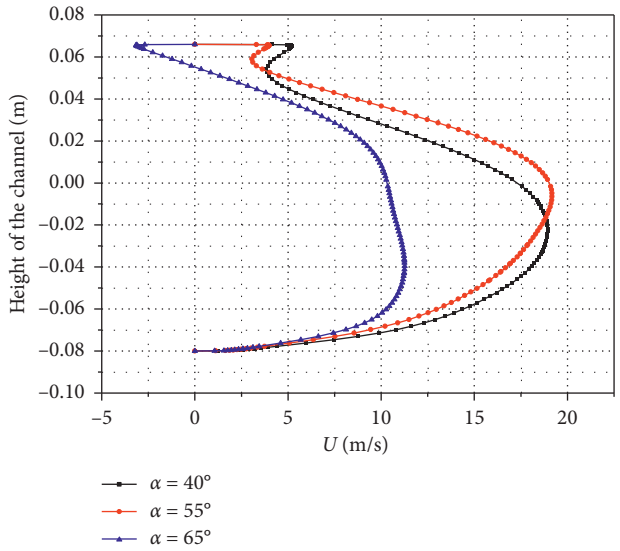

Figure 9: Axial velocity profiles upstream of the second baffle at $x = 0.345$ m for different values of inclination angles: $\varphi_1 = 40^\circ$; $\varphi_2 = 55^\circ$; $\varphi_3 = 65^\circ$.

In addition, the results of velocity profiles are depicted in Figures 8 and 9 for the different values of inclination angles (cases a, b, and c), in the areas upstream of the second baffle defined by the positions: $x = 0.315$ m and $x = 0.345$ m. The dynamic results obtained show that the velocity decreases in the lower part of the channel, while in the upper part it increases. Thus, we note the existence of a large difference in the maximum velocity for the three treated cases, whereas in the area near the channel outlet, the value of the maximum axial velocity is about four times the value of the axial velocity at the inlet (see Figure 10) where the results are calculated at the position ($x = 0.525$ m).

Thus, in the lower part of the channel, we observed that the fluid flow accelerated versus the reduction of inclination angles and become relatively reversed in the downstream of the baffle. This is due to the sensitivity of the dynamic comportment of the fluid downstream of the second baffle.

4.3. Heat Transfer. Figure 11 shows the distribution of the local friction coefficient along the channel for the three cases. The result shows that the local friction coefficient on the walls varies slightly in the absence of obstacles,

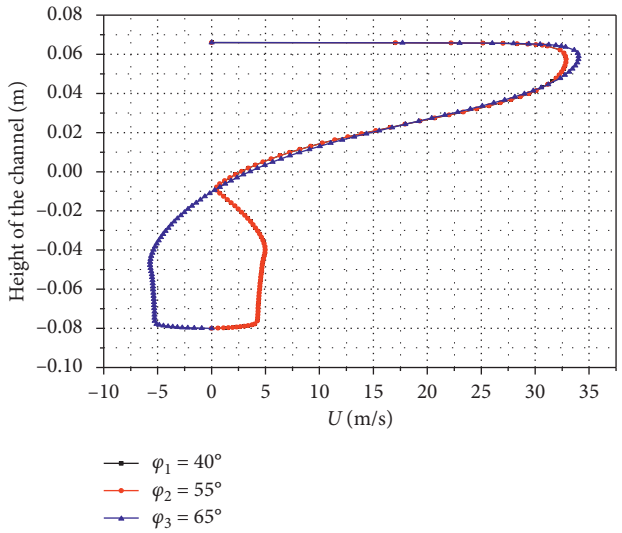

FIGURE 10: Axial velocity profiles near the exit of channel at $x = 0.525$ m for different values of inclination angles: $\varphi_1 = 40^\circ$; $\varphi_2 = 55^\circ$; $\varphi_3 = 65^\circ$.

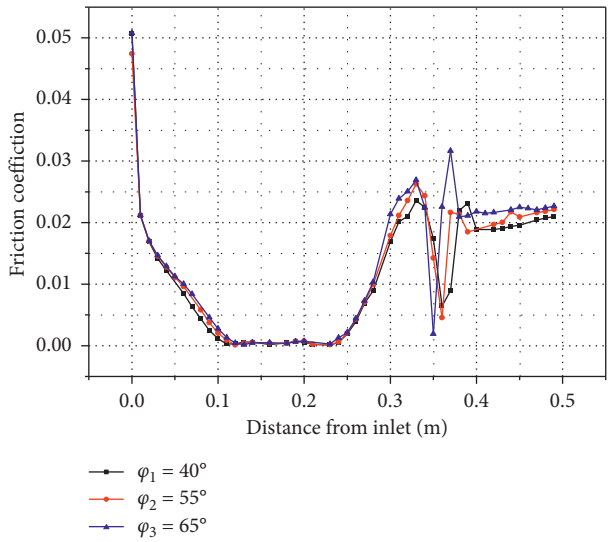

FIGURE 11: Variation of friction coefficient along upper channel wall for $\varphi_1 = 40^\circ$, $\varphi_2 = 55^\circ$, and $\varphi_3 = 65^\circ$.

upstream of the first baffle. On the other hand, the results show that the friction coefficient importantly increases between the two baffles and outlet of the channel. This is because the fluid has no space for circulating quickly in downstream of the baffle. Thus, there is the formation of recirculation zones. It has also been noticed that the high values of the local friction coefficient are located downstream of the second baffle. This was manifested by the orientation of the flow by the second baffle to the walls of the channel with high-velocity intensities. Therefore, the increases of inclination angle affect the increase of the pressure drop. In fact, the results allow us to conclude that the friction coefficient increases with increase in inclination angle of the baffles.

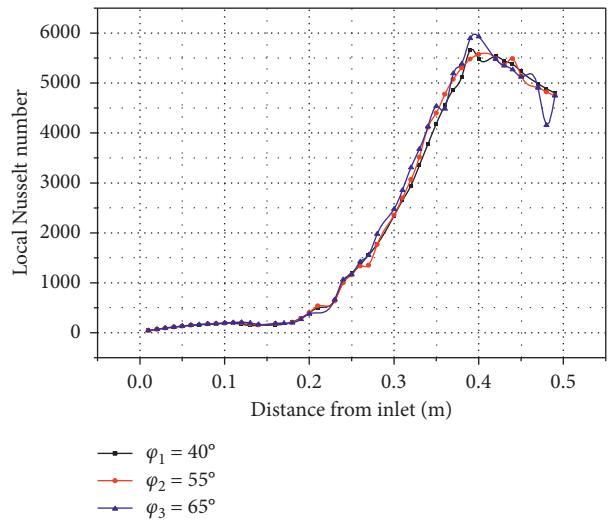

FIGURE 12: Distribution of the local Nusselt number along upper channel wall for $\varphi_1 = 40^\circ$, $\varphi_2 = 55^\circ$, and $\varphi_3 = 65^\circ$.

Local Nusselt number Nu in the presence of the two baffles placed on the upper and lower walls with spacing L_1 and for different values of inclination angles (cases a, b, and c) is shown in Figure 12. The results obtained show the important effect of inclination angle of the baffles on heat transfer along the channel compared to the smooth channel. These results show that the heat transfer upstream of the first baffle ($x < 0.2$ m) is low for the three studied cases and that the curves are almost confused in this region. In addition, a complete change of the behavior of Nu is observed in the field between the baffles and upstream of the second baffle. There is a remarkable variation in the Nusselt number along the channel with a significant difference between the curves representing the three cases. In particular, just after the position of the first baffle, the effect of the inclination baffle on the local Nusselt number becomes progressively important.

Finally, in all cases, downstream of position defined by $x = 0.23$ m, the variation in the Nusselt number along the channel is significant. This variation of Nu presents a maximum value of heat transfer at position $x = 0.42$ m in which corresponding to the position of second baffle and thereafter remains constant to the exit of the channel.

5. Conclusions

The present paper is dedicated to a numerical analysis using the finite volume method on turbulent forced convection in a partitioned channel. In light of the results discussed, the main determination can be summarized as follows:

(i) The heat transfer and flow structure are considerably affected by the variation in inclination angle of the partitions.

(ii) The maximum inclusive heat transfer of the channel is realized when the inclination angle increases;

thence, the inclination of baffles could be an interesting method to improve the thermal performance of the heat exchanger.

(iii) The distribution of local friction coefficient is positively affected by inclination angle $\varphi_3 = 65^\circ$.

Abbreviations

CFD: Computational fluid dynamics
CPU: Central processing unit
DCB: Discrete combined baffles
FVM: Finite volume method
LBM: Lattice Boltzmann method
QUICK: Quadratic interpolation for convective kinetics
SIMPLE: Semi-implicit method for pressure linked equation
THE: Tube heat exchanger

Symbols

C_f: Friction Coefficient
D_h: Hydraulic diameter, (m)
H: Height of the channel, (m)
h: Height of the baffle, (m)
h_x: Heat transfer coefficient ($W/m^2 \cdot K$)
k: Turbulent kinetic energy
L: Length of the channel, (m)
L_1: Distance between inlet of the channel and the first baffle, (m)
L_2: Distance between the two baffles, (m)
L_3: The distance between the second baffle and outlet of the channel, (m)
Nu: Local Nusselt number
Pr: Prandtl Number, ($Pr = 0.7$)
Q: Heat flux at position along the channel
Re: Reynolds Number
T_{int}: Inlet temperature, (K)
T_w: Wall temperature, (K)
T: Temperature (K)
U_{in}: Velocity of air at inlet of the channel, (m/s)
U, V: Cartesian components of velocity, (m/s)
U_{int}: Inlet velocity, (m/s)
x, y: Dimensional Cartesian coordinates, (m)

Greek letters

ε: Dissipation rate of turbulence energy
τ: Shear stress, (Pa)
μ_t: Turbulent viscosity, (Pa·s)
λ_f: Thermal conductivity of fluid, ($W \cdot m^{-1} \cdot K^{-1}$)
ρ: Air density (kg/m^3)
φ: Inclination angle (degree)
ϕ: Generic variable
μ: Dynamic viscosity of the fluid, (Kg/m·s)
ν: Kinematic viscosity, (m^2/s)
δ: Thickness of the baffle, (m).

Data Availability

No data were used to support this study.

Conflicts of Interest

The authors declare that there are no conflicts of interest regarding the publication of this article.

References

[1] E. Vishnuvardhanarao and M. K. Das, "Mixed convection in a buoyancy-assisted two-sided lid-driven cavity filled with a porous medium," *International Journal of Numerical Methods for Heat & Fluid Flow*, vol. 19, no. 3/4, pp. 329–351, 2009.

[2] M. Ozturk, "Energy and exergy analysis of a combined ground source heat pump system," *Applied Thermal Engineering*, vol. 73, no. 1, pp. 362–370, 2014.

[3] F. Menasria, M. Zedairia, and A. Moummi, "Numerical study of thermohydraulic performance of solar air heater duct equipped with novel continuous rectangular baffles with high aspect ratio," *Energy*, vol. 133, pp. 593–608, 2017.

[4] R. K. Tiwari and M. K. Das, "Heat transfer augmentation in a two-sided lid-driven differentially heated square cavity utilizing nanofluids," *International Journal of Heat and Mass Transfer*, vol. 50, no. 9-10, pp. 2002–2018, 2007.

[5] H. Yang, P. Cui, and Z. Fang, "Vertical-borehole ground-coupled heat pumps: a review of models and systems," *Applied Energy*, vol. 87, no. 1, pp. 16–27, 2010.

[6] H. Ma, D. E. Oztekin, S. Bayraktar, S. Yayla, and A. Oztekin, "Computational fluid dynamics and heat transfer analysis for a novel heat exchanger," *Journal of Heat Transfer*, vol. 137, no. 5, 2015.

[7] K. Milani Shirvan, S. Mirzakhanlari, S. A. Kalogirou, H. F. Öztop, and M. Mamourian, "Heat transfer and sensitivity analysis in a double pipe heat exchanger filled with porous medium," *International Journal of Thermal Sciences*, vol. 121, pp. 124–137, 2017.

[8] M. Siavashi, H. R. Talesh Bahrami, and E. Aminian, "Optimization of heat transfer enhancement and pumping power of a heat exchanger tube using nanofluid with gradient and multi-layered porous foams," *Applied Thermal Engineering*, vol. 138, pp. 465–474, 2018.

[9] Y. Dahani, A. Amahmid, M. Hasnaoui et al., "Effect of nanoparticles on the hysteresis loop in mixed convection within a two-sided lid-driven inclined cavity filled with a nanofluid," *Heat Transfer Engineering*, vol. 40, no. 1-2, pp. 128–146, 2018.

[10] A. Andreozzi, "Numerical study of mixed convection in a horizontal no parallel-plates channel with an unheated moving plate," *International Journal of Numerical Methods for Heat & Fluid Flow*, vol. 28, no. 3, pp. 547–570, 2018.

[11] K. Amghar, M. A. Louhibi, N. Salhi, and M. Salhi, "Numerical simulation of forced convection turbulent in a channel with transverse baffles," *Journal of Materials and Environmental Science*, vol. 8, pp. 1417–1427, 2017.

[12] K. Amghar, M. A. Louhibi, H. Bouali, N. Salhi, and M. Salhi, "Turbulent forced convection heat transfer in a horizontal partitioned channel," *Lecture Notes in Electrical Engineering*, vol. 519, pp. 1–9, 2019.

[13] H. Benzenine, R. Saim, S. Abboudi, O. Imine, H. F. Oztop, and N. Abu-Hamdeh, "Numerical study of a three-dimensional forced laminar flow in a channel equipped with a perforated baffle," *Numerical Heat Transfer, Part A: Applications*, vol. 73, no. 12, pp. 881–894, 2018.

[14] D. Sahel, H. Ameur, R. Benzeguir, and Y. Kamla, "Enhancement of heat transfer in a rectangular channel with perforated baffles," *Applied Thermal Engineering*, vol. 101, pp. 156–164, 2016.

[15] R. Saim, H. Benzenine, H. F. Öztop, and K. Al-Salem, "Turbulent flow and heat transfer enhancement of forced convection over heated baffles in a channel," *International Journal of Numerical Methods for Heat & Fluid Flow*, vol. 23, no. 4, pp. 613–633, 2013.

[16] Y. Menni, A. Azzi, and A. Chamkha, "Enhancement of convective heat transfer in smooth air channels with wall-mounted obstacles in the flow path," *Journal of Thermal Analysis and Calorimetry*, vol. 135, no. 4, pp. 1951–1976, 2018.

[17] H. Ameur, "Effect of corrugated baffles on the flow and thermal fields in a channel heat exchanger," *Journal of Applied and Computational Mechanics*, vol. 6, no. 2, pp. 209–218, 2019.

[18] H. Ameur, "Effect of the baffle inclination on the flow and thermal fields in channel heat exchangers," *Results in Engineering*, vol. 3, Article ID 100021, 2019.

[19] A. Boonloi and W. Jedsadaratanachai, "Numerical investigation on turbulent forced convection and heat transfer characteristic in a square channel with discrete combined V-baffle and V-orifice," *Case Studies in Thermal Engineering*, vol. 8, pp. 226–235, 2016.

[20] D. Sahel, H. Ameur, and B. Touhami, "Effect of the size of graded baffles on the performance of channel heat exchangers," *Thermal Science*, vol. 6, p. 295, 2018.

[21] H. Ameur and Y. Menni, "Laminar cooling of shear thinning fluids in horizontal and baffled tubes: effect of perforation in baffles," *Thermal Science and Engineering Progress*, vol. 14, Article ID 100430, 2019.

[22] L. C. Demartini, H. A. Vielmo, and S. V. Möller, "Numeric and experimental analysis of the turbulent flow through a channel with baffle plates," *Journal of the Brazilian Society of Mechanical Sciences and Engineering*, vol. 26, no. 2, pp. 153–159, 2004.

[23] B. E. Launder and D. B. Spalding, "The numerical computation of turbulent flows," *Computer Methods in Applied Mechanics and Engineering*, vol. 3, no. 2, pp. 269–289, 1974.

[24] T.-H. Shih, W. W. Liou, A. Shabbir, Z. Yang, and J. Zhu, "A new k-ϵ eddy viscosity model for high Reynolds number turbulent flows," *Computers & Fluids*, vol. 24, no. 3, pp. 227–238, 1995.

[25] Nasiruddin and M. H. K. Siddiqui, "Heat transfer augmentation in a heat exchanger tube using a baffle," *International Journal of Heat and Fluid Flow*, vol. 28, no. 2, pp. 318–328, 2007.

[26] S. V. Patankar, "Numerical heat transfer and fluid flow," *Series in Computational Methods in Mechanics and Thermal Sciences*, Hemisphere Publishing Corporation, New York, NY, USA, 1980.

[27] A. Boonloi and W. Jedsadaratanachai, "Numerical study on flow and heat transfer mechanisms in the heat exchanger channel with V-orifice at various blockage ratios, gap spacing ratios, and flow directions," *Modelling and Simulation in Engineering*, vol. 2019, Article ID 061102, 21 pages, 2019.